VOL. 9, NO. 8, AUGUST 2014 ISSN 1819-6608
ARPN Journal of Engineering and Applied Sciences


www.arpnjournals.com

IDENTIFICATION AND LOCATION OF FAULT ON A TRANSMISSION LINE USING WAVELET BASED ON CLARKE'S TRANSFORMATION

Makmur Saini[1, 2], Abdullah Asuhaimi Bin Mohd Zin[1], Mohd Wazir Bin Mustafa[1] and Ahmad Rizal Sultan[1, 2]
[1]Faculty of Electrical Engineering, UniversitiTeknologi Malaysia, UTM Johor Bahru, Malaysia
[2]Politeknik Negeri Ujung Pandang, South Sulawesi, Indonesia
E-Mail: makmur.saini@fkegraduate.utm.my

ABSTRACT

This paper presents a study on fault detection and location by using PSCAD to obtain the current signal in the transformation of signal interference. This study was done by using the Clarke's transformation method to transfer the current signal phase (three phase) signal into a two-phase current, alpha current and gamma current (current Mode). New method with fault current approach is introduced in this paper. Mode current in transform signal using discrete wavelet transform (DWT) was utilized to obtain the wavelet transform coefficients *(WTC)* [2], to determine the current time when the disturbance amplitude values *(WTC)* [2] reached a maximum point value. Mother wavelet was used to compare the Db4, Sym4, Coil4 and Db8. The fault location was determined using the Clarke transformation, then transformed into wavelet, which was very accurate and thorough. Analysis was also conducted for some other mother wavelets. The error of the simulated wavelet fourth parent was found less than 2%. The most accurate parent was wavelet Db8 with the fastest time of detection and the most minor error, whereas the largest error was found in the parent wavelet Coil4.

Keywords: wavelet transformation, fault location, fault detection, Clarke's transformation.

1. INTRODUCTION

Fault detection and purpose of the location of short circuit transmission line have become a growing apprehension. There are two methods commonly used to conclude the location in agreement with standard IEEE StdC37.114. 2004 [IEEE]. The first method is based on frequency component, and the second method is based on signal intrusion at high frequencies and ignores the wave theory, and uses a shorter sampling window (H.P. Magnago. *at al*., 1998). The strength of mind of wave theory for interference detection was first used by (H.W. Dommel. *at al*., 1979), where a graph pattern was described by using the transient voltage waveform, and the current waveform was used to determine the fault detection and fault location.

C.Y. Evrenosoglu. *at al*., (2005) then industrial a circuit that passed the technical relationship between the arrival of peak measurement-to-point, and the forward and backward traveling waves were used to predict the travel time of a transient signal transmitter (source signal) to the point affected by the fault. Wave theory is categorized under graphic patterns (M.M. Saha. *at al*., 2010). They are described based on the voltage waveform and current waveform, in the form of a brief association between the entrance of the peak value at the measurement point of forward and backward waves.

This paper presents a different approach, which is based on Clarke's transformation, or also called as alpha-beta transformation. It is the transformation of a three-phase system (a, b, c) into a two-phase (alpha beta) (B. Polajzer. *at al*., 2006), in which the result of transient two-phase flow is then transformed into wavelet.

Wavelet transform (WT) is a technique to solve the signal problem, based on the development of Fourier transformation (Chaari. *at al*., 1997).WT has the privilege of able to map a set of functions when these areas are at the time scaling region. The basic functions used in wavelet transform have a band pass characteristic that makes mapping similar to the mapping in the form of time - frequency (S. Patthi. *at al*., 2012).

The basic functions used in the Fourier analysis are limited only by the frequency, whereas the wavelets are not limited to only the frequency but also including sudden disturbances such as a transient disturbance. The wavelets generate waves and disrupt the signal frequency (S.R. Samantaray. *at al*., 2008).

The application of WT to analyze transient signals in the electric power system is known to have a number of benefits (C. Kim. *at al*., 2001). This paper presents an overview comparison of Fourier; short-time Fourier and wavelet transform, which are the several examples for the application of WT to analyze transient power system.

Computer simulations were performed using PSCAD / EMTDC (PSCAD Manual), which produced a transient signal interference from the transmission line simulation with a sampling rate (10^5) in one type of disorder. The data were then transferred into MATLAB with the help of Clarke's transformation to convert the three-phase signals into the two-phase signal, after the wavelet had been transformed into its parent. Several other types such as Db4 wavelet, Sym4, Coil4 and Db8 were compared to determine the timing of the interference with the transmission line.

2. OVERVIEW OF CLARKE'S AND WAVELET TRANSFORMATION

2.1. Clarke's transformation

Clarke's transformation, or also referred as ($\alpha\beta$) transformation, is a mathematical transformation that is used to simplify the analysis of a series of three phases (a,

b, c). It is a two-phase circuit (αβ0) stationery and theoretically very similar to the (dqo) transformation. The wave signal analyzer is a very useful application for the transformation.

Clarke, s transformation is one of the transformation matrix which corresponds to the three-phase transmission lines, in application as a phase-mode transformation matrix. Un-transposed three-phase transmission lines have been analyzed through the comparison of the error and frequency. For un-transposed under asymmetric three-phase transmission line real sample, the correction procedure is applied for searching for better results than Clarke application matrix as phase-mode transformation matrix. A three-phase current which has a digital representation is assumed to have the form (O.F. Alfredo. *at al*., 2008)

$$i_a(n) = I_a \cos(n\omega T + \varphi a)$$
$$i_b(n) = I_b \cos(n\omega T + \varphi b)$$
$$i_c(n) = I_c \cos(n\omega T + \varphi c) \quad (1)$$

where T is the sampling period.

Equation (1) can be put into the following matrix form. Therefore, the above components can be formed in a matrix form (A.J. Prado. *at al*., 2006)

$$i_{mode}=i_{\alpha\beta 0}=Ci_{abc}=\frac{2}{3}\begin{bmatrix}1 & -\frac{1}{2} & -\frac{1}{2}\\ 0 & \frac{\sqrt{3}}{2} & -\frac{\sqrt{3}}{2}\\ \frac{1}{2} & \frac{1}{2} & \frac{1}{2}\end{bmatrix}x\begin{bmatrix}i_a\\ i_b\\ i_c\end{bmatrix} \quad (2)$$

where C the famous transformation introduced by [(Edith Clarke. 1950)], which functions to convert the three phase currents system (a, b, c) into a two-phase (alpha beta)

2.2. Wavelet transformation

Wavelet transformation is a modification of the Fourier transformation, with one important difference, in which the wavelet transform allows placement time as the frequency components within the given different signal. Sort Time Fourier Transforms (STFT) is another improvement of Fourier transform (E.S.T. Eldin. *at al*., 2007)], which uses a fixed amount of the modulation window. This is due to the narrow window that gives a bad time resolution. Therefore, the Fourier transform is only suitable for the information signal frequency as it does not change according to time.

In wavelet analysis, the functions will be adjusted so that the time window of the wavelet frequency with higher frequency will be very narrow, and the wavelets with lower frequency will be widespread. Wavelet transformation has several features that make it particularly suitable for this particular application, unlike the basic functions used in Fourier's analysis. The wavelets are not only limited to the frequency but also in time. This placement takes into account of the detection time of the incident disturbances that may occur suddenly as a transient disturbance. The two wavelet transforms are CWT and DWT.

2.2.1. Continuous wavelet transformation

The continuous wavelet transform (CWT) is used to calculate the intricacy of a signal from a modulation signal, with a window at any time to any desired scale. Scale window has a flexible modulation. By giving a wave function f (t), the CWT can be calculated as follows [B.Ibrahem. *at al*., 2011)

$$\text{CWT (f,a,b)}=\frac{1}{\sqrt{a}}\int_{-s}^{s} f(t)\varphi^{*}\left(\frac{t-b}{a}\right)dt \quad (3)$$

where a and b are the constants and constant scale translational, CWT (f, a, b) is the CWT of a coefficient, and φ is the unreal other wavelet. The selection of the parent wavelet will be adapted to the needs of the wavelet coefficients. The input signal *f(t)* is rearranged by using a shift parameter and the time dilation of the right scale.

2.2.2. Discrete wavelet transformation

Discrete wavelet transform (DWT) is measured as a relatively easy to be implemented compared with a CWT. The basic principle of DWT is determining how to obtain the timing and scale a representation of a signal using a digital preservation technique and sub-sampling operation. Coefficient of DWT of a wave can be obtained by applying the DWT. The coefficient of DWT of a wave can be obtained by applying the DWT as given by the equation (H. Eristi. *at al*., 2012)

$$\text{DWT (f.m.k)} =\frac{1}{\sqrt{a_0^m}}\sum_k f(k)\varphi^{*}\left[\frac{n-ka_0^m}{a_0^m}\right] \quad (4)$$

where the parameters a and b in the equation (4) are replaced as $a_o m$, ka_o^m , where k and m are positive integer variables. From just a few samples of WTC taken, the implementation of DWT decomposition is essentially based on a Mallat algorithm (S.G. Malla. 1989), The wave input signal is separated into two parts, namely the low-frequency signals called approximation and detailed high-frequency section.

Mother wavelet transform has various stems of Daubechies, Symlet and Coiflet. The most widely used transformation is the transformation of normal stem Daubechies, with written DbN; where N is the sequence of events, and b shows the Daubechies mother wavelet (D. Chandra. *at al*., 2003), with high value of N discrete sample.

3. RESEARCH METHOD

The simulations were performed using PSCAD, and the simulation results were obtained from the fault current signal.

The steps performed for this study were:

a) Decision the input to the Clarke transformation and wavelet transformation, the signal flow of PSCAD

transformed into m.files (*. M) and then to be converted into mat. files (*mat).with a sampling rate (10^5) and frequency charge 0.5 Hz - 1 MHz .

b) Formative the data stream intervention, where the signal was changed by using the Clarke transformation to convert the transient signals into the signals basic current (Mode).

c) Mode current signals were transformed again by using DWT and WTC, which was the generated coefficient and then squared to be $(WTC)^2$ in order to obtain the maximum signal amplitude to determine the timing of the interruption.

d) Handing out the ground mode and aerial mode an $(WTC)^2$ using Bewley Lattice diagram (Datta *at al*., 2012) of the initial wave to determine the fault location

e) Fault detection and fault location flowchart as shown in Figure-1.

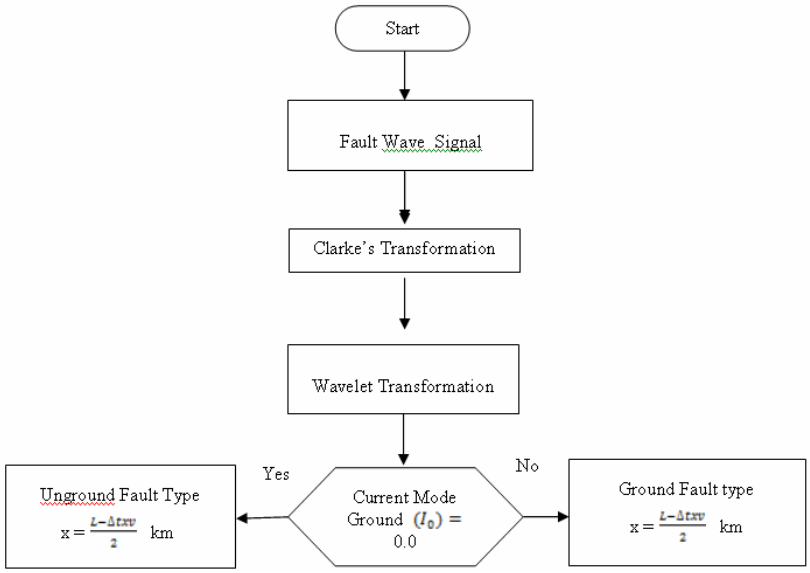

Figure-1. Fault detection and fault location flowchart.

4. THE SIMULATION RESULTS AND DISCUSSIONS

Single circuit transmission line connected with the sources at each end, as shown in Figure-2. This system was simulated using PSCAD/EMTD for the case study; the simulation was modeled on a 150 kV single circuit Transmission line.

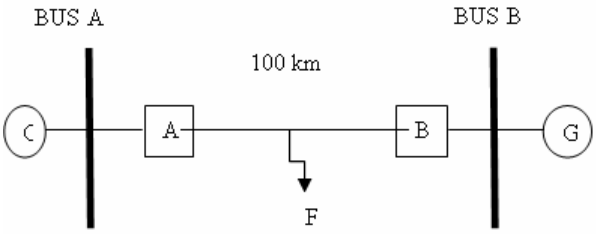

Figure-2. Single circuit transmission line using PSCAD/EMTDC.

Sequence Impedance ohm/km
Positive and negative = 0.03574 + j 0.5776
Zero = 0.36315 + j 1.32.647
Fault Starting = 0.22 seconds
Duration in fault = 0.15 seconds
Fault resistance (R_f) = 2 ohm

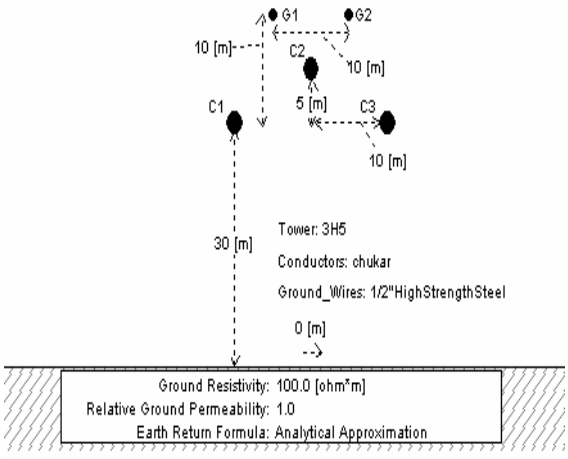

Figure-3. Three-phase line configuration.

Type Conductor = Chukar, diameter = 1.602 inch.

The results of calculations were taken into account of the position of the tower and the distance between the conductors as shown in Figure-3. The conductor types used for this simulation were obtained

using propagation velocity $= \frac{1}{\sqrt{LC}}$ = 299939.4321 km/second. (See Appendix)

4.1. Case-1: Line to line to ground fault (ACG), 50 km from bus A and 50 km from bus B

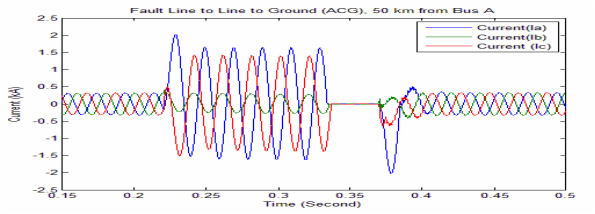

(a). Current waveform signal original

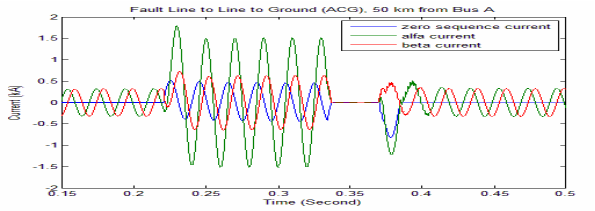

(b). Current mode waveform from Clarke's transformation

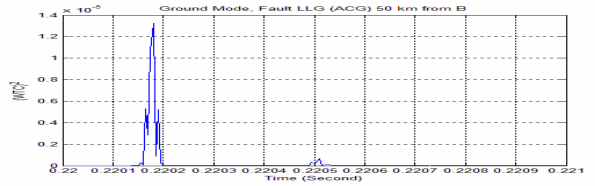

(c). Ground mode for wavelet mother Db4

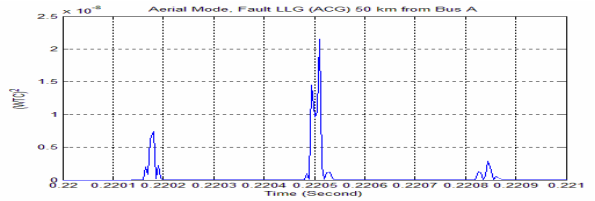

(d). Aerial mode for wavelet mother Db4

Figure-4. Line to line to ground fault (ACG) 50 km from bus A for case-3.

Figure-4 (a) presents the transient signal interference from Bus A. The resulting fault current interruption of bus A to point as far as 50 km was Ia = 2.024 kA, Ib= 0.4027 kA and Ic = 1.429 kA. Figure-4 (b) shows the current mode signal with $I\alpha$ = 1.794 kA, $I\beta$ = 1.193 and Io = 0.517 kA from bus A to point disorder at 50 km from Figure-4 (b) with Io = 0.517 kA, so that the disorder would be a ground fault. Figure-4 (c) shows the graph $(WTC)^2$ in ground mode. The results of wavelet transformation in which the value of existing ground to the height of mode showed tA = 0.2218 second showed that this disorder type was ground fault. Figure-4 (d) shows the graph $(WTC)^2$ in Aerial mode, in which the first peak occurred at $(WTC)^2$ at tA= 0.22018 second.

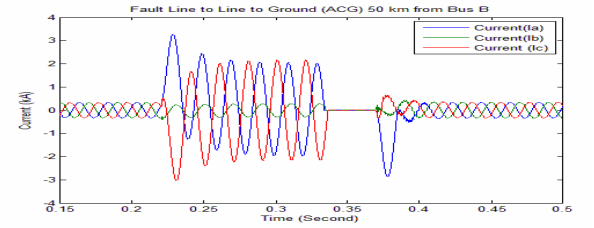

(a). Current waveform signal original

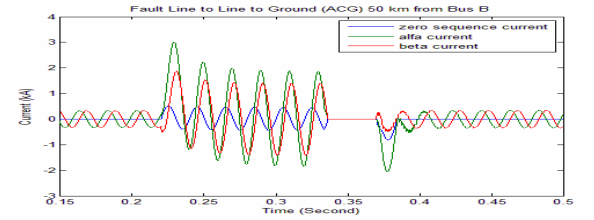

(b). Current mode waveform from Clarke's transformation

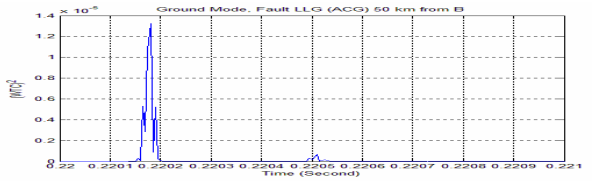

(c). Ground mode for wavelet mother Db4

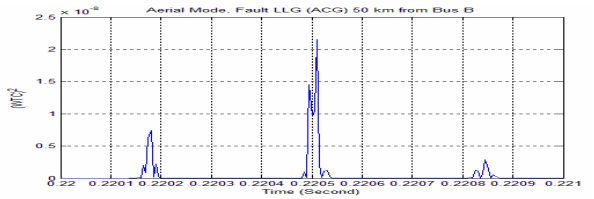

(d). Aerial mode for wavelet mother Db4

Figure-5. Line to line ground fault (ACG) 50 km from bus B for case-3.

Figure-5(a) shows the transient interference signals measured from bus B, which was obtained from the bus fault current interruption to point B at 50 km, with Ia = 3.273 kA, Ib= 0.4403kA and Ic = 2.167 kA. Figure-5 (b) shows a graph of the signal mode with current $I\alpha$ = 3.140 kA, $I\beta$ = 1.877 kA and Io = 0.517 kA of bus B to point of interruption at 75 km, from the current Figure-5 (b) above, in which Io = 0.517 kA so that interference would be a ground fault. Figure-5 (c) shows a $(WTC)^2$ graph in ground mode, where the wavelet transform results indicated that the value type was a ground-fault interference with the first peak occurring at 0.22018second. Figure-5 (d) shows $(WTC)^2$ graphs on fashion aerial where a peak $(WTC)^2$ occurred at tB = 0.22018This can be seen in Figure-6, the calculation percentage of the error line to line ground fault (ACG).

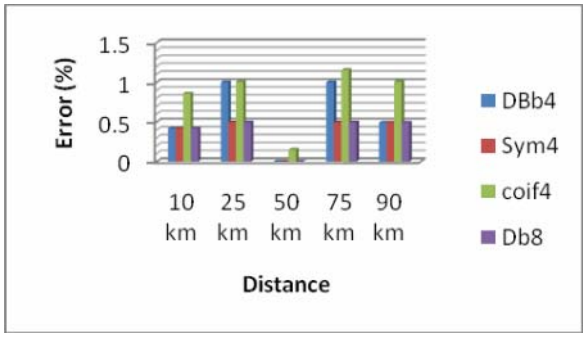

Figure-6. Error of line to line ground fault (ACG) for case-3.

In Figur-6 the calculation percentage of the error fault line to line to ground shows that at 10 km and 90 km, long transmission lines Db4, Sym4 and Db8 had the same percentage of error. On the other hand, at 25 km and 75 km, the percentage error of Sym4 and Db8 were lesser compared with Db4 and Coif4 since Coif4 had a major percentage of error in all cases. For 50 km, the percentage of error was better compared to others.

4.2. Case-2: Three-phase fault (ABC), 90 km from bus A and 10 km from bus B

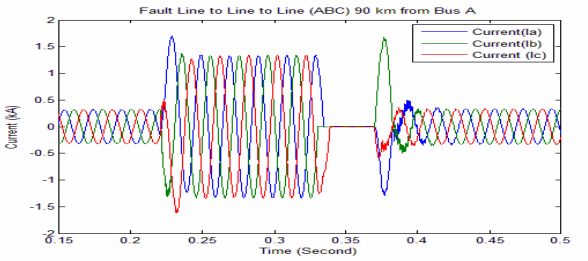

(a). Current waveform signal original

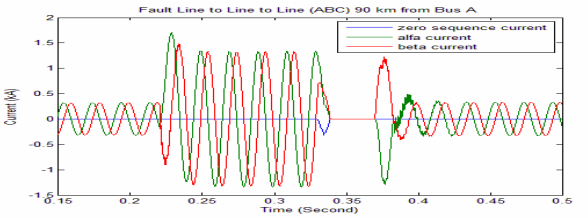

(b). Current mode waveform from Clarke's transformation

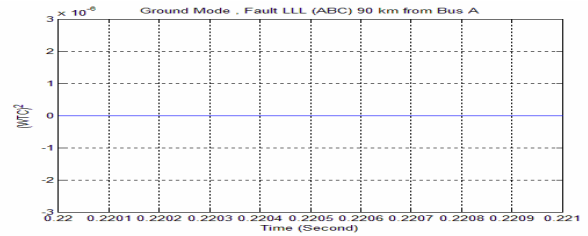

(c). Ground mode for wavelet mother Coil4

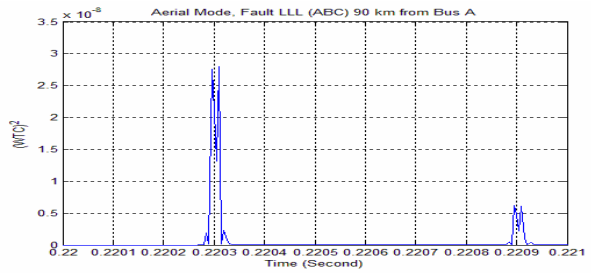

(d). Aerial mode for wavelet mother Coil4

Figure-7. Three-phase phase fault (ABC) 90 km from bus A case-4.

Figure-7(a) shows the transient interference signals measured from Bus A. The fault current was obtained from Bus A to the point of interruption at 90 km Ia = 1.704 kA, Ib= 1.674 kA and Ic = 1.337 kA. Figure-7 (b) shows a graph mode signal current signal obtained, which were $I\alpha$ = 1.704 kA, $I\beta$ = 1.483 kA and Io = 0 from bus A to disorder point at 90 km. Figure-7 (b) shows that the current Io = 0. Therefore, it can be concluded that there was a disruption of ungrounded fault. Figure-7 (c) shows a $(WTC)^2$ graph in ground mode. The results of wavelet transformation, in value of ground zero mode, showed that this type of interference was ungrounded fault. Figure-7 (d) shows $(WTC)^2$ graph in Aerial mode where the peak occurred at $(WTC)^2$ at tA= 0.2203 second.

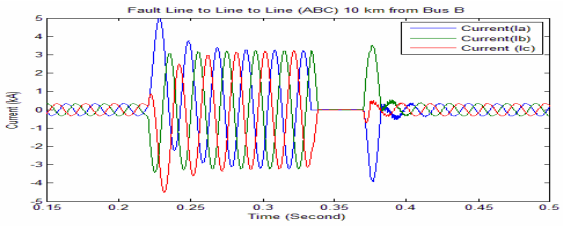

(a). Current waveform signal original

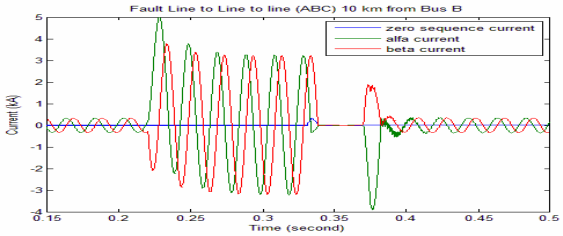

(b). Current mode waveform from Clarke's transformation

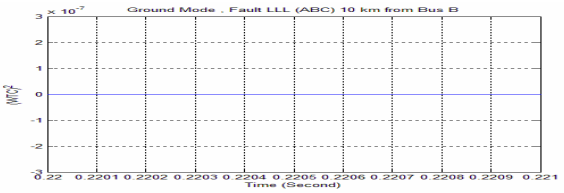

(c). Ground mode for wavelet mother Coil4

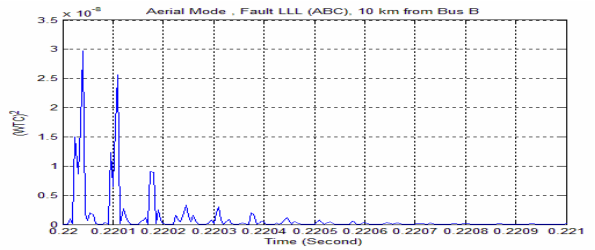

(d). Aerial mode for wavelet mother Coil4

Figure-8. Three-phase fault 10 km from bus B for case-4.

Figure-8(a) presents the transient signal interference from Bus B, obtained from the bus fault current interruption to point B at 10 km, with *Ia* = 4.998 kA, *Ib* = 3.523 kA and *Ic*= 3.224 kA. Figure-8 (b) shows a graph of the signal mode with current *Iα* = 4.998 kA *Iβ* = 0.3784 kA and *Io* = 0 on bus B to point disorder as far as 10 km. Figure-8 (b) shows that *Io* = 0. Therefore, it can be concluded that the interference type was an ungrounded fault. Figure-8 (c) shows a $(WTC)^2$ graph on ground mode, where the result of wavelet transformation was the ground mode = zero values, which means this disorder type was an ungrounded fault. Figure-8 (d) shows the graph $(WTC)^2$ in Aerial mode in which the peak occurred at$(WTC)^2$ at *tB* = 0.220035 second.

Figure-9 shows the calculated error for three-phase fault (ABC).

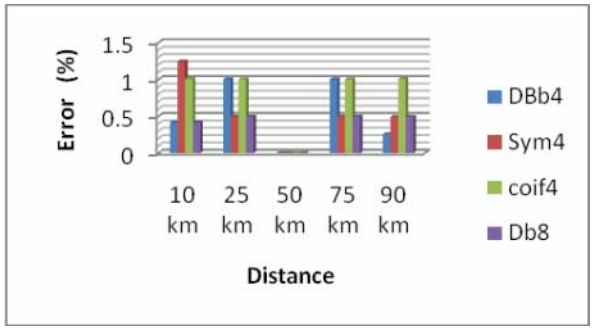

Figure-9. Error three phase fault (ABC) case-4.

Figure-9 shows that percentage of error for 10 km, Db4 and Db8 were the same, but the Sym4 had the highest percentage of error compared with others. In case of at 25 km and 75 km, Sym4 and Db8 had lesser errors compared with Db4 and Coif4. Meanwhile, in case of at 90 km, Db4 was better compared to others, while the position at 50 km had the best of all cases compared to 10 km, 25 km, 75 km and 90 km.

5. CONCLUSIONS

This paper presents a new wavelet transform based fault location method, by using the Clarke's transformation method to convert the current signal phase (three phase) signal into a two-phase current, alpha current and gamma current was very accurate and thorough, with an error less than 2%, even at a distance of the same 50 km disorder, with an average error of 0.2%, in which achieve the time of bus A to the point of disorder time of the achieved by bus B. From the above results, Db8 was found the best compared with other mother wavelets, with the fastest detection time of 0.000165 seconds and created the smallest error in all types of interference. In the intervening time, the largest percentage error was created by the mother wavelet Coif4.

ACKNOWLEDGEMENT

The authors would like to express their gratitude to Universiti Teknologi Malaysia, The State Polytechnic of Ujung Pandang, PT. PLN (Persero) of South Sulawesi and the Government of South Sulawesi Indonesia for providing the financial and technical support for this research.

APPENDIX

Propagation velocity of chukar conductor see Figure-4

Propagation velocity = $\frac{1}{\sqrt{LC}}$

L = $2*10^{-7}$ ln $\frac{D_{eg}}{D_s}$ H/m /phasa

C = $\frac{2\pi k}{\ln(\frac{D_{eg}}{D_s})}$ F/m / phasa

k = $8.85\ 10^{-12}$ F/m

$D_{eg} = \sqrt[3]{D_{ab} D_{bc} D_{ca}}$

$D_s = r\, e^{-\frac{1}{4}}$

r = 1.602 inch = 2.0345 cm (chukar Conductor)

$D_{eg} = \sqrt[3]{20 * 11.18 * 11.18}$

$D_{eg} = 13.5718\ meter$

D_{eg} = $2.0345\ 10^{-3} e^{-\frac{1}{4}}$ = $1.5573\ 10^{-3}$ meter

L = $2*10^{-7}$ ln $\frac{13,5718}{1.5573*10^{-3}}$ = $1.814559 * 10^{-6}$ H/m

C= $\frac{2*\pi*8.85*10^{-12}}{\ln\frac{13.5718}{1.5573*10^{-3}}}$ = $6.125785 * 10^{-12}$ F/m

$\vartheta_i = \frac{1}{\sqrt{LC}} = \frac{1}{\sqrt{1.814559*10^{-6}*6.125785*10^{-12}}}$ = 299939, 4321 km/second

REFERENCES

A.J. Prado, J.P. Filho, S. Kurokawa and L.F. Bovolato. 2005. Non-transposed three-phase line analyses with a single real transformation matrix. The 2005 IEEE/Power Engineering Society General Meeting, CD-ROM 12-16 June, San Francisco, USA.

B. Ibrahem, Z. Inmaculada, M. Javier and B. Garikoitz. 2011. High impedance fault detection methodology using wavelet transform and artificial neural networks. Electric Power Systems. Res. 81: 1325-1333.

B. Polajzer, G. S. Tumberger, S. Seme, D. Dolinar. 2008. Detection of voltage sources based on instantaneous voltage and current vectors and orthogonal clarke's transformation. IET. Gener. Transm. Distrib. 2(2): 219-226.

Chaari M. and Meunier F. Brouave. 1997. Wavelet new tool for the resonant grounded power distribution systems relaying. IEEE Trans. on Power Delivery. 11(3): 1301-1308.

C. Kim and R. Aggarwal. 2001. Wavelet transform in power systems. Power Eng. J. 15 (4): 193-202.

C.Y. Evrenosoglu and A. Abur. 2005. Fault location in Distribution System with Distribution Generation. 15th PSCC. 10(5): 1-5.

Datta A. Rajagopal. 2012. Literature review on use bewley's lattice diagram. Power and Energy in Nerist (ICPEN), India.

D. Chandra and N.K. Kishore, A. Sinha. 2003 . A Wavelet multiresolution analysis for location of fault on transmission line. Electrical Power and Energy System. 25: 59-69.

E. Clarke. 1950. Circuit Analysis of AC Power Systems. Vol. I. Wiley, New York, USA.

E.S.T. Eldin, D.K. Ibrahim, E.M. Abdul Sahap and S.M. Saleh. 2007. High Impedance Fault Detection in EHV Transmission Line using Wavelet Transform. Power Engineering Society General Meeting IEEE: 1-7.

F.H. Magnago and A. Abur. 1998. Fault location using wavelets. IEEE Transactions on Power Delivery. 13(4): 1475-1480.

H. Eristi and Y. Demir. 2012. Determinant-based feature extraction for fault detection and classification for power transmission lines. IET Gener. Transm. Distrib. 6(10): 968-976.

H.W. Dommel and J.M. Michels, 1978. High speed relaying using traveling wave transient analysis. IEEE Publications No. 78CH1295-5 PWR. Paper No. A78 214-9, IEEE PES Winter Power Meeting, New York, USA, 1-7.

IEEE Guide for Determining Fault Location on AC Transmission and Distribution Lines. 2004. IEEE Std. C37.114, General Meeting, CD-ROM 12-16 June, San Francisco, USA.

M.M. Saha, J. Izykowski and E. Rosolowski. 2010. Fault location on power network. Spinger. pp. 22-25.

O.F. Alfredo, I.E. Luis and R.E. Carlos. 2006. Three-phase adaptive frequency measurement based on Clarke's Transformation. IEEE Trans. on Power Delivery. 21(3): 1101-1105.

PSCAD/EMTDC User's Manual. 2001. Manitoba HVDC Research Center. Winnipeg, MB, Canada.

S.G. Malla. 1989. Theory for multiresolution signal decomposition the wavelet representation. IEEE Tran Pattern Anal Mach Intell. 11(7): 794-798.

S. Patthi, P.S. Birendra and V.K.R. Pulapa. 2012. Neutral current wave shape analysis using wavelet for diagnosis of winding insulation of a transformer. Turk J. Elec Eng and Comp Sci. 20: 835-841.

S.R. Samantaray and P.K. Dash. 2012. Transmission line distance relaying using a variable window short-time Fourier transform. Electric Power Systems Research. 78: 595-604.